

中国激光

窄线宽蓝光半导体激光器研究

王渴^{1,2}, 韩金樑^{1,2}, 梁金华³, 单肖楠^{1*}, 王立军¹

¹中国科学院长春光学精密机械与物理研究所, 吉林 长春 130033;

²中国科学院大学, 北京 100049;

³吉林省长光瑞思激光技术有限公司, 吉林 长春 130051

摘要 由于有色金属对蓝光激光光源具有良好的吸收效率,因此蓝光半导体激光器逐步成为研究热点。针对激光加工纯铜、纯金、高强铝等高反射金属材料的市场需求,采用体布拉格光栅作为外腔反馈元件,压窄激光线宽,稳定激光波长,并基于空间合束技术将6片单管蓝光激光芯片聚焦耦合进芯径为105 μm、数值孔径为0.22的光纤中,研制出窄线宽蓝光半导体激光光纤耦合模块。当工作电流为3 A时,该激光模块的输出功率为26.32 W,稳定输出波长为444.29 nm,光谱线宽被压至0.18 nm。

关键词 激光器; 蓝光半导体激光器; 窄线宽; 体布拉格光栅; 外腔反馈

中图分类号 TN248.4 文献标志码 A

DOI: 10.3788/CJL220925

1 引言

随着激光加工技术的不断发展和工业需求的不断提高,短波长蓝光激光逐步成为激光器领域的研究热点。蓝光波长通常在400~500 nm范围内,具有波长短、衍射效应小、能量高等特性,蓝光半导体激光器在贵金属激光加工、量子通信、激光显示、激光美容、增材制造等领域^[1-3]有着广阔的应用前景。

工业上通常采用红外激光进行金属加工,但铜、金、铝等有色金属材料具有高反射率^[4],对红外波长激光的吸收效果较差。激光照射金属材料,大部分能量被反射,同时被照射部分的能量会快速传递到周围,造成金属材料及合金切割困难。传统红外激光器不仅体积大、操作复杂,同时还需要较高功率运作以及复杂的冷却装置。采用蓝光半导体激光器解决以纯铜、纯金、高强铝为代表的高反射高导热材料的激光加工问题是近些年来的研究热点。

近年来,为了研究窄线宽半导体激光输出,以不同光栅作为外腔反馈元件的半导体激光器常见报道。Ding等^[5]报道了一种窄线宽的高功率 Littrow 型外腔蓝光激光器,在1100 mA 电流下线宽约为0.1 nm,输出功率为1.24 W。Mukhtar等^[6]报道了一种外腔二极管激光器(ECDL),在130 mA 电流下线宽≤110 pm,输出功率为14.5 mW。李斌等^[7]报道了基于反射式全息光栅的405 nm 蓝紫光半导体激光器,在19.7 mA 和21.3 mA 阈值电流下谱线宽度为0.03 nm。然而,这些

报道多是基于 Littrow 布局的光栅外腔半导体激光器,基于体布拉格光栅的瓦级高功率蓝光半导体激光器的综合性能研究鲜有报道。自由运转的蓝光单元芯片的光谱线宽通常为1 nm,无法满足光谱合束^[8-10]的要求,因此需要通过技术手段压窄蓝光激光线宽,同时稳定激光的输出波长。

针对贵金属激光加工领域对高功率蓝光激光器的需求,本文选用外腔光反馈法,极大改善了激光器的输出线宽。采用多个单管蓝光芯片,基于反射式体布拉格光栅(RVBG)外腔反馈技术、激光空间合束技术^[11-12]及光纤耦合技术,获得了功率为26.32 W、线宽为0.18 nm、光纤芯径为105 μm的蓝光激光输出。

2 实验原理及设计

采用基于GaN的蓝光半导体激光器(LD)作为单元器件,表1列出了所用的蓝光激光二极管(LD)的主要参数。由于LD单管输出功率有限,需要利用多单管空间合束技术获得激光高功率输出。如图1所示,采用阶梯式的空间排布结构,摆放6片波长为447 nm的蓝光芯片,阶梯高度为0.4 mm,保证激光束互不干扰。其中,单管蓝光芯片集成在次热沉基底上,保证了蓝光LD的功率稳定性高、寿命长及可靠性好的优势;通过RVBG对空间合束后的激光束进行波长锁定及线宽压窄,改善输出光谱特性;将激光束耦合进芯径为105 μm、数值孔径(NA)为0.22的光纤中,提高蓝光激光光束质量。

收稿日期: 2022-06-01; 修回日期: 2022-06-23; 录用日期: 2022-07-18; 网络首发日期: 2022-07-28

基金项目: 吉林省科技厅发展计划项目(20190302048GX)、广东省重点领域研发计划(2020B090922002)、吉林省科技发展计划(20210209062RQ)

通信作者: *shanaxiaon@sina.com

表 1 单管蓝光 LD 的主要参数

Table 1 Main parameters of single tube blue LD

Parameter	Value
Center wavelength / nm	447
Output power / W	5
Operating current / A	3
Operating voltage / V	4.3
Slow axis divergence angle / (°)	10
Fast axis divergence angle / (°)	60
Cavity length / mm	1.2

激光光束质量是评价合束系统的重要指标,通常采用光参数积(B)来评价^[13]。定义为光斑的束腰半径($D/2$)与远场发散半角(θ)的乘积:

$$B = \frac{D}{2} \times \theta。 \quad (1)$$

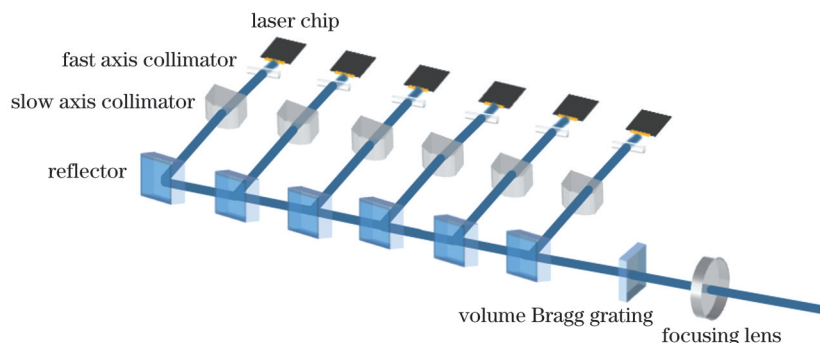


图 1 实验装置的内部布局
Fig. 1 Internal layout of experimental device

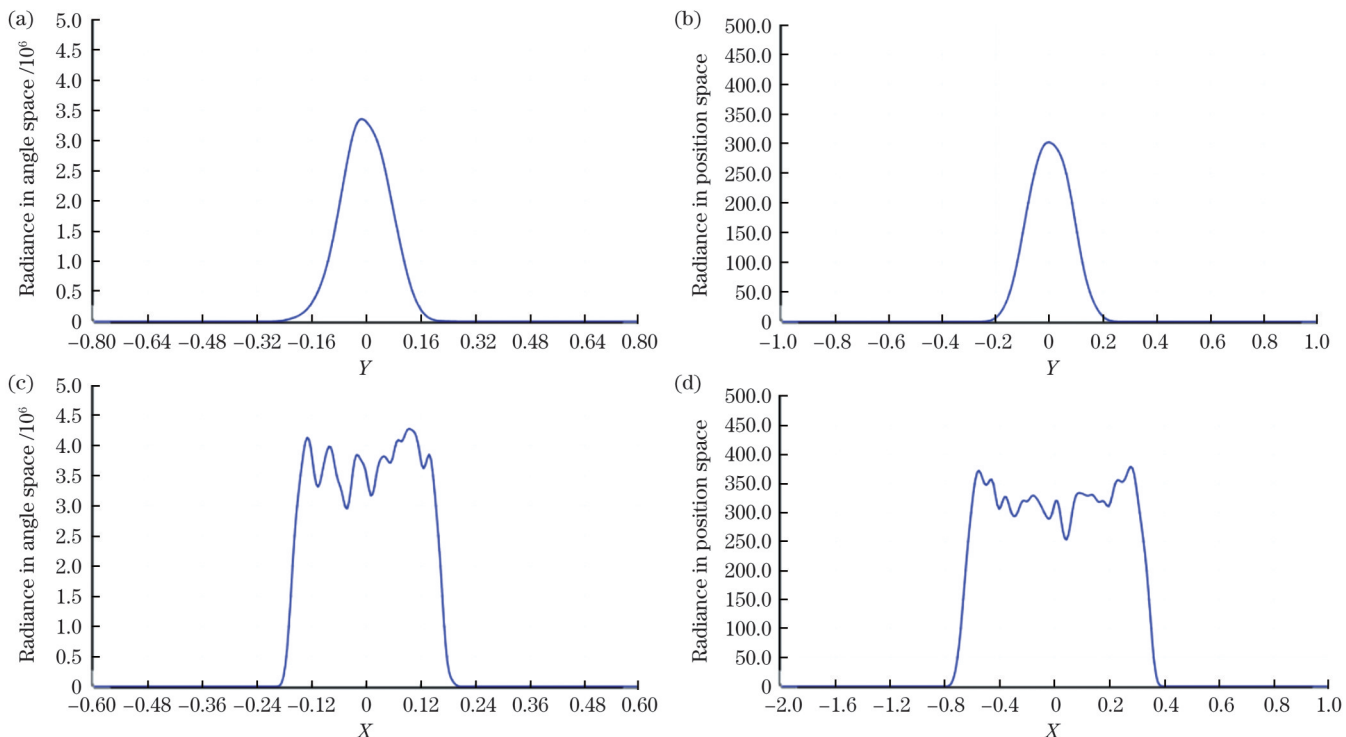


图 2 单芯片准直后的发散角和光斑尺寸。(a)快轴发散角;(b)快轴光斑尺寸;(c)慢轴发散角;(d)慢轴光斑尺寸
Fig. 2 Divergence angles and spot sizes after single chip collimation. (a) Fast axis divergence angle; (b) fast axis spot size; (c) slow axis divergence angle; (d) slow axis spot size

的值越小,表示激光光束质量越好。

LD 单管快、慢轴方向的发散角不同且有很大的发散特性,由表 1 可得,LD 单管在快轴方向的发散角为 60° ,慢轴方向的发散角为 10° ,快轴方向发散角远大于慢轴方向,需要在合束处理之前对 LD 单管分别进行快、慢轴准直处理。通过 Zemax 软件进行模拟仿真,快轴准直镜(FAC)选用焦距为 0.31 mm 的非球面柱面镜,FAC 准直后快轴方向的发散角半角为 2.1 mrad ,光斑尺寸为 0.36 mm ,如图 2(a)、(b)所示,对应的光参量积为 $0.378\text{ mm}\cdot\text{mrad}$;慢轴准直镜(SAC)采用焦距为 9.3 mm 的柱面镜,SAC 准直后慢轴方向的发散角半角为 2.8 mrad ,光斑尺寸为 1.6 mm ,如图 2(c)、(d)所示,对应的光参量积为 $2.24\text{ mm}\cdot\text{mrad}$ 。光学准直后激光快、慢轴的发散角显著减小,保证了光束的传输质量。

为了增大激光输出功率,采用空间合束技术紧密排列组合光束,将 6 片蓝光芯片按照阶梯型排列以压缩光束间距,空间合束后的激光光斑如图 3 所示,光斑尺寸为 $1.6 \text{ mm} \times 2.4 \text{ mm}$ ($X \times Y$)。此时,合束后的快、慢轴光参数积为

$$B_{\text{slow}} = \frac{D_{\text{slow}}}{2} \times \theta_{\text{slow}} = \\ 0.8 \text{ mm} \times 2.8 \text{ mrad} = 2.24 \text{ mm} \cdot \text{mrad}, \quad (2)$$

$$B_{\text{fast}} = \frac{D_{\text{fast}}}{2} \times \theta_{\text{fast}} = \\ 1.2 \text{ mm} \times 2.1 \text{ mrad} = 2.52 \text{ mm} \cdot \text{mrad}, \quad (3)$$

式中: B_{fast} 、 B_{slow} 分别为快、慢轴光参数积; D_{fast} 、 D_{slow} 分别为快、慢轴光斑直径; θ_{fast} 、 θ_{slow} 分别为快、慢轴发散半角。

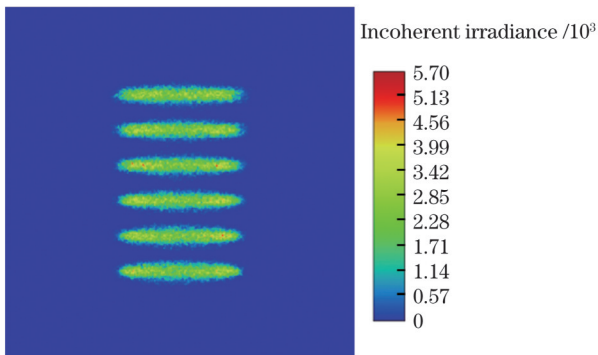


图 3 空间合束后的光斑图

Fig. 3 Spot diagram after space beam combination

空间合束后,在光学系统中加入 RVBG,对合束激光进行同步外腔反馈,从而达到锁定波长、压窄光谱线宽的

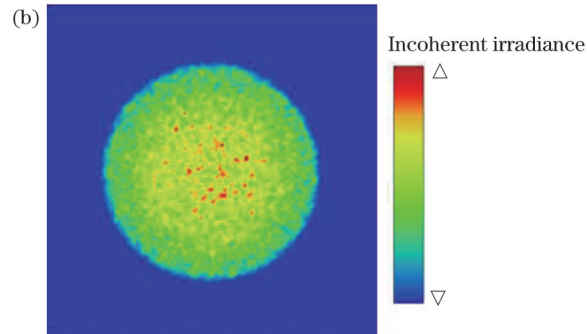
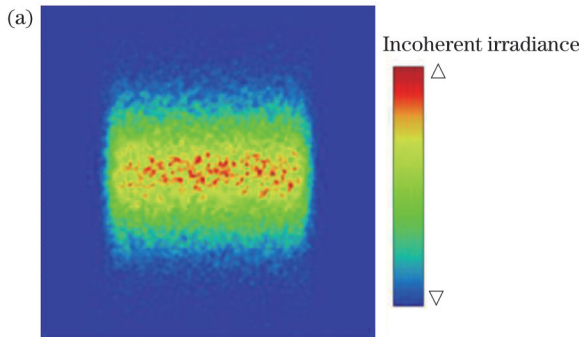


图 4 光斑图。(a) 聚焦光斑图;(b) 光纤耦合后光斑图

Fig. 4 Spot diagrams. (a) Focused spot diagram; (b) spot diagram after optical fiber coupling

3 实验结果与分析

RVBG 外腔结构的一个重要作用就是改善输出光谱特性。在 3.0 A 工作电流(I)下,图 5(a)为单个蓝光芯片在自由运转下的输出光谱,图 5(b)为单个芯片发射出的激光通过 RVBG 后的输出光谱,输出波长锁定在 444.07 nm 附近。由图 5 可知,RVBG 外腔结构明显改善了输出蓝光的光谱特性,光谱谱宽从 1.39 nm 被压窄到约 0.18 nm。

采用 RVBG 作为反馈元件构建窄线宽蓝光半导

目的,所用 RVBG 的衍射效率为 15%±3%,衍射波长为 (443.8 ± 0.1) nm。在通常情况下,自由运转激光器各发光单元的输出波长存在差异,导致输出光束谱线较宽;同时它们易受外界环境温度的影响,这进一步影响了自由运转半导体激光的光谱特性。RVBG 作为外腔光反馈元件,可以将特定波长的光重新反馈回出光区,降低该波长的光损耗,有利于该波长的模式竞争,使得激光器输出单一波长模式,实现外腔对波长的锁定^[14-15]。

外腔反馈后的激光再经过聚焦镜耦合到光纤中进行传输。为了使合束后的激光束耦合进芯径为 105 μm、数值孔径为 0.22 的光纤中,根据光纤耦合条件^[16-17]可知,聚焦后的光斑尺寸不大于光纤芯径,聚焦后的光斑发散角不大于光纤数值孔径,即

$$D_{\text{laser}} < D_{\text{fiber}}, \quad (4)$$

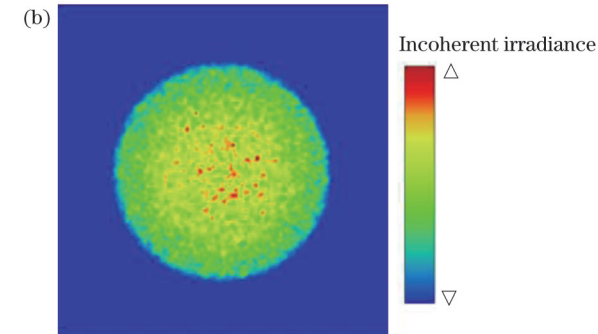
$$\theta_{\text{laser}} < \theta_{\text{fiber}} = 2 \arcsin(NA), \quad (5)$$

式中: D_{laser} 为聚焦后的光斑直径; θ_{laser} 为光束聚焦后的远场发散全角; D_{fiber} 为光纤芯径; θ_{fiber} 为数值孔径为 0.22 的光纤对应的最大入射角。

$$f \leq \frac{D_{\text{fiber}}}{\sqrt{\theta_{\text{fast}}^2 + \theta_{\text{slow}}^2}}, \quad (6)$$

式中: f 为聚焦镜焦距。

通过式(6)计算确定聚焦镜的焦距范围为 $f \leq 15$ mm,选取焦距为 12 mm 的商用聚焦镜,经过模拟耦合效率可达 99% 以上。图 4(a)是聚焦透镜聚焦后的光斑图,图 4(b)是激光束从光纤输出后的近场光斑图,可见光强分布更均匀。



体激光器,如图 6 所示。在水冷温度为 20 °C 时,自由运转的蓝光芯片的阈值电流为 0.6 A,6 路出光的功率为 1.26 W;加入体布拉格光栅(VBG)外腔反馈后,蓝光芯片的阈值电流降低到 0.5 A,6 路出光的功率为 1.38 W。当工作电流提高到 3.0 A 时,激光合束后的输出功率为 29.4 W,RVBG 外腔反馈后的输出功率为 29.87 W,反馈效率达到 101.6%,这是由于 VBG 外腔反馈后激光输出阈值功率降低。在光谱锁定方面,图 7(a)为 3.0 A 电流下 RVBG 锁模前的光谱图,显示有多个峰值。图 7(b)为 3.0 A 电流下 RVBG 锁模后的

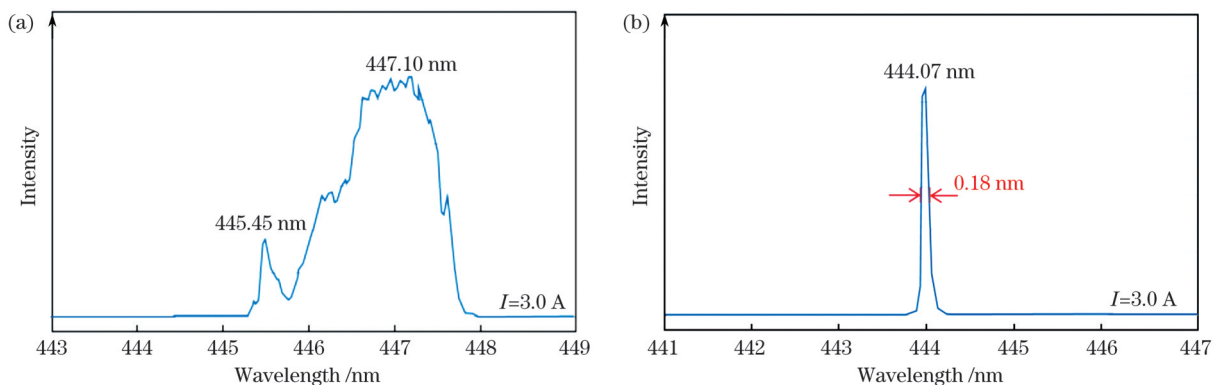


图 5 单个蓝光芯片的输出光谱图。(a)RVBG 锁模前;(b)RVBG 锁模后

Fig. 5 Output spectra of single blue laser chip. (a) Before RVBG mode locking; (b) after RVBG mode locking

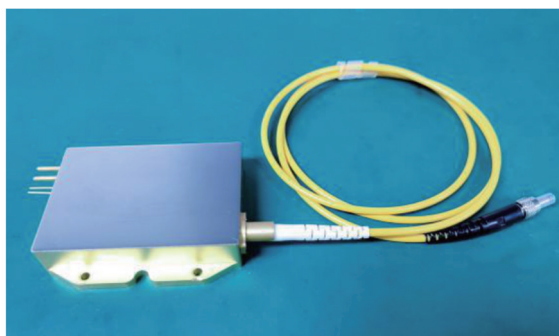


图 6 蓝光激光器模块实物图

Fig. 6 Physical picture of blue laser module

光谱图,可以清晰看出锁模效果明显,输出为单一波长模式,锁定波长为 444.29 nm,光谱线宽压缩到 0.18 nm 左右。

边模抑制比(S_M)是主模强度和边模强度的最大值之比,是表征纵模性能的一个重要指标:

$$S_M = 10 \lg (I_0/I_1), \quad (7)$$

式中: I_0 表示主模峰值强度; I_1 表示除主模峰值强度外的边模最大强度。蓝光半导体激光器压窄后的光谱主峰强度与次峰强度的比约为 30:1,即 $S_M=14.78$ dB。该测试结果表明,通过 VBG 对自由运转的蓝光激光器进行外腔反馈,获得了很好的线宽压窄效果。

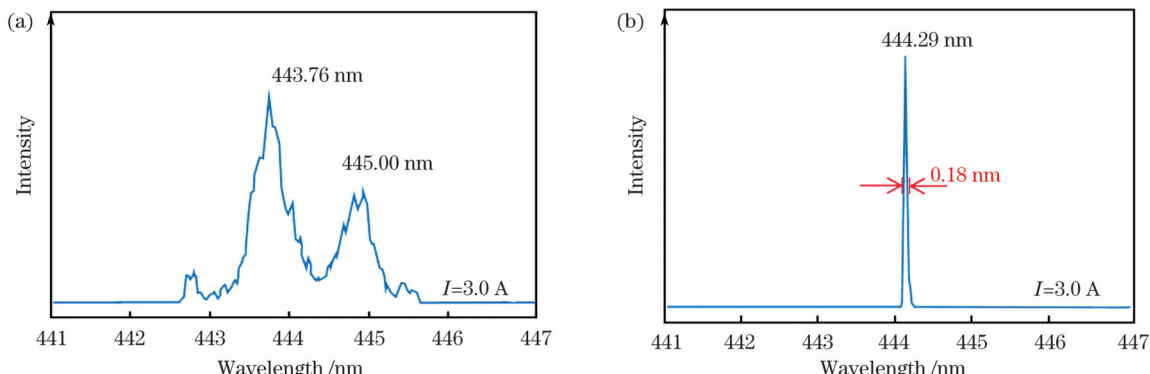


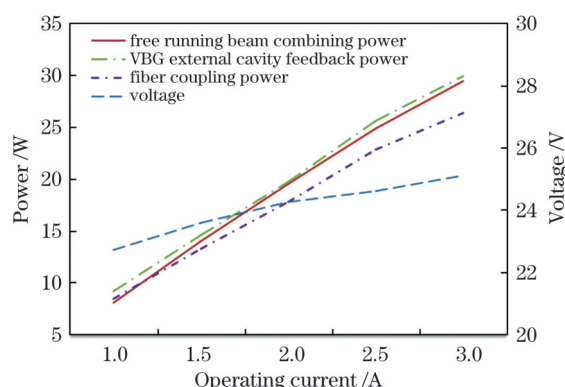
图 7 蓝光激光器模块的输出光谱图。(a)RVBG 锁模前;(b)RVBG 锁模后

Fig. 7 Output spectra of blue laser module. (a) Before RVBG mode locking; (b) after RVBG mode locking

图 8 为窄线宽蓝光耦合模块的功率-电流-电压(P - I - V)测试曲线图。在连续条件下,整个激光器在驱动电流 0~3.0 A 范围内调节,当工作电流增加至 3.0 A 时,电压为 25.1 V,从芯径为 105 μm、数值孔径为 0.22 的光纤中获得 26.32 W 的输出功率,电光转换效率为 34.95%,对应耦合效率为

$$\eta = \frac{P_{\text{fiber}}}{P_{\text{foc}}} = \frac{26.32}{29.87} \times 100\% = 88.1\%, \quad (8)$$

式中: P_{fiber} 为光纤耦合后的输出功率; P_{foc} 为光纤耦合前的输出功率。在实际操作中,激光器装调完成后的耦合效率比仿真模拟值低,这是实验中的人为误差、工艺误差或整体装调误差等导致的。

图 8 模块的 P - I - V 曲线Fig. 8 P - I - V curves of module

4 结 论

采用反射式体布拉格光栅作为反馈元件,搭建了蓝光外腔半导体激光器,结合空间合束、光纤耦合技术,获得了高功率、窄线宽、稳光谱的激光输出,其中输出功率为 26.32 W,稳定输出波长为 444.29 nm,光谱线宽被窄化为 0.18 nm,光纤耦合效率达到 88.1%。后续将进一步通过实验研究,减少耦合损耗,提升光谱锁定质量,再结合光谱合束技术,获得更高功率的蓝光半导体激光器。

参 考 文 献

- [1] 吴鹏. 百瓦级高功率蓝光半导体激光器研究[D]. 北京: 北京工业大学, 2017.
Wu P. Study on 100 W level high-power blue diode laser[D]. Beijing: Beijing University of Technology, 2017.
- [2] Li X H, Liu X M, Gong Y K, et al. A novel erbium/ytterbium co-doped distributed feedback fiber laser with single-polarization and unidirectional output[J]. Laser Physics Letters, 2010, 7(1): 55-59.
- [3] Li X H, Wang Y G, Wang Y S, et al. Yb-doped passively mode-locked fiber laser based on a single wall carbon nanotubes wallpaper absorber[J]. Optics & Laser Technology, 2013, 47: 144-147.
- [4] 顾波. 高功率蓝光半导体激光器为金属加工打开了新的大门[J]. 金属加工(热加工), 2021(3): 1-6.
Gu B. High power blue-light semiconductor laser has opened a new door for metal processing[J]. MW Metal Forming, 2021(3): 1-6.
- [5] Ding D, Lü X Q, Chen X Y, et al. Tunable high-power blue external cavity semiconductor laser[J]. Optics & Laser Technology, 2017, 94: 1-5.
- [6] Mukhtar S, Ashry I, Shen C, et al. Blue laser diode system with an enhanced wavelength tuning range[J]. IEEE Photonics Journal, 2020, 12(2): 1502110.
- [7] 李斌, 高俊, 赵俊, 等. 宽调谐范围光栅外腔窄线宽 405 nm 蓝紫光半导体激光器研究[J]. 中国激光, 2015, 42(12): 1202003.
Li B, Gao J, Zhao J, et al. Study on broad tuning range and narrow line-width 405 nm blue-violet diode laser with grating external cavity[J]. Chinese Journal of Lasers, 2015, 42(12): 1202003.
- [8] 张志军. 大功率半导体激光器合束技术及应用研究[D]. 长春: 中国科学院长春光学精密机械与物理研究所, 2013.
Zhang Z J. Research on high-power semiconductor laser beam combiner technology and application[D]. Changchun: Changchun Institute of Optics, Fine Mechanics and Physics, Chinese Academy of Sciences, 2013.
- [9] Zediker M S, Fritz R D, Finuf M J, et al. Laser welding components for electric vehicles with a high-power blue laser system[J]. Journal of Laser Applications, 2020, 32(2): 022038.
- [10] 张俊, 彭航宇, 付喜宏, 等. 基于光谱合束的 800 nm 高亮度半导体激光源[J]. 中国激光, 2020, 47(7): 0701021.
Zhang J, Peng H Y, Fu X H, et al. High-brightness 800-nm semiconductor laser source based on spectral beam combining[J]. Chinese Journal of Lasers, 2020, 47(7): 0701021.
- [11] 宁永强, 陈泳屹, 张俊, 等. 大功率半导体激光器发展及相关技术概述[J]. 光学学报, 2021, 41(1): 0114001.
Ning Y Q, Chen Y Y, Zhang J, et al. Brief review of development and techniques for high power semiconductor lasers[J]. Acta Optica Sinica, 2021, 41(1): 0114001.
- [12] 韩金樑, 张俊, 单肖楠, 等. 基于半导体激光合束技术的高效点火光源研究[J]. 中国激光, 2022, 49(7): 0701002.
Han J L, Zhang J, Shan X N, et al. High-efficiency ignition laser source based on diode laser beam combination technology[J]. Chinese Journal of Lasers, 2022, 49(7): 0701002.
- [13] 朱洪波, 郝明伟, 刘云, 等. 808 nm 高亮度半导体激光器光纤耦合器件[J]. 光学精密工程, 2012, 20(8): 1684-1690.
Zhu H B, Hao M M, Liu Y, et al. 808 nm high brightness module of fiber coupled diode laser[J]. Optics and Precision Engineering, 2012, 20(8): 1684-1690.
- [14] Zhu H B, Fan S L, Zhao J, et al. Development and thermal management of kW-class high-power diode laser source based on the structure of two-stage combination[J]. IEEE Photonics Journal, 2019, 11(3): 1502510.
- [15] Ishige Y, Hashimoto H, Hayamizu N, et al. Blue laser-assisted kW-class CW NIR fiber laser system for high-quality copper welding[J]. Proceedings of SPIE, 2021, 11668: 116680M.
- [16] Baumann M, Balck A, Malchus J, et al. 1000 W blue fiber-coupled diode-laser emitting at 450 nm[J]. Proceedings of SPIE, 2019, 10900: 1090005.
- [17] 段程芮, 赵鹏飞, 王旭葆, 等. 高亮度蓝光半导体激光器光纤耦合技术[J]. 光电工程, 2021, 48(5): 49-56.
Duan C R, Zhao P F, Wang X B, et al. Fiber coupling technology of high brightness blue laser diode[J]. Opto-Electronic Engineering, 2021, 48(5): 49-56.

Research on Narrow Linewidth Blue Semiconductor Laser

Wang Ke^{1,2}, Han Jinliang^{1,2}, Liang Jinhua³, Shan Xiaonan^{1*}, Wang Lijun¹

¹Changchun Institute of Optics, Fine Mechanics and Physics, Chinese Academy of Sciences, Changchun 130033, Jilin, China;

²University of Chinese Academy of Sciences, Beijing 100049, China;

³Jilin Changguang Ruisi Laser Technology Co., Ltd., Changchun 130051, Jilin, China

Abstract

Objective Continuous progress in laser processing technology and its growing industrial demand have resulted in short-wavelength blue lasers gradually becoming a research hotspot in the field of laser research. Blue semiconductor lasers have broad application prospects in precious-metal laser processing, laser-based cosmetic treatments, additive manufacturing, and other fields. Infrared lasers are usually used for metal processing in industry; however, owing to the high reflectivity of non-ferrous metals such as copper, gold, and aluminum in materials, the absorption effect of infrared wavelength lasers is low. In addition, conventional infrared lasers are bulky and complicated to operate and require high-power operation and complex cooling devices. The use of blue semiconductor lasers as a solution to process materials with high reflectivity and high thermal conductivity, such as pure copper, pure gold, and high-strength aluminum, has become a popular research topic in recent years. In addition, the spectral line width of a free-running blue

light unit chip is usually 1 nm, which does not satisfy the requirements for spectral beam combination. Therefore, it is necessary to reduce the line width of blue light laser by technical means and simultaneously stabilize the output wavelength of the laser.

Methods This paper proposes a blue laser with a narrow line width. First, we present the structural design of multiple single-tube blue semiconductor lasers. The design entails coupling multiple 447 nm blue light chips to form an optical fiber with core diameter of 105 μm and numerical aperture of 0.22 using spatial combination technology and the feasibility of this solution is verified by simulation using ZEMAX optical design software. Second, the laser line width is effectively narrowed using a reflective volume Bragg grating (RVBG). Because the output wavelength of each light-emitting unit of the free-running laser is different, the spectral line width of the output beam is increased. Therefore, the RVBG acts as an external cavity optical feedback element to enable the laser to output a single wavelength mode; in addition, the external cavity also serves to lock the wavelength. Finally, the narrow line width enables blue semiconductor lasers to deliver high-power performance, which can be detected from the optical path structure with the use of spectrometers. This lays the technical foundation for the practical realization of high-power blue lasers.

Results and Discussions A photographic image of the output light source of the blue semiconductor laser is shown in Fig. 4. When the operating current is set to 3.0 A, the output spectrum of a single chip is stably locked at a wavelength centered at 444.07 nm after the light passes through the RVBG external cavity (Fig. 5). In terms of laser power, when the water-cooling temperature is 20 °C, the threshold current of the free-running blue light chip is 0.6 A, and the six channels can output 1.26 W laser. After the addition of volume Bragg grating (V BG) external cavity feedback, the threshold is reduced to 0.5 A, and the six channels can output 1.38 W laser. Upon increasing the working current to 3.0 A, the output power is increased to 29.4 W after combining the laser beams. After RVBG external cavity feedback, the output power is 29.87 W, and the feedback efficiency reaches 101.6%. This is owing to the reduction in laser output threshold power after the addition of V BG external cavity feedback. In terms of spectral locking, multiple peak states exist in the spectrum before RVBG mode locking for a current of 3.0 A. After locking the RVBG mode, the mode-locking effect is clearly observed. The output is a single wavelength mode, the locked wavelength is 444.29 nm, and the spectral line width is narrowed to about 0.18 nm (Fig. 7). The module for narrow-line-width blue light coupling passes the power-current-voltage test. Under continuous conditions, the entire laser is adjusted within the driving current range of 0–3.0 A. When the operating current is increased to 3.0 A, the voltage is 25.1 V, and the output power of 26.32 W is obtained from the fiber with a core diameter of 105 μm and numerical aperture of 0.22. The electro-optical conversion efficiency is 34.95%, corresponding to a coupling efficiency of 88.1% (Fig. 8).

Conclusions The RVBG is used as the feedback element to build a blue-light external-cavity semiconductor laser. Using spatial beam combination and fiber coupling technology, a laser output with a high power, narrow line width, and stable spectrum is obtained. The output power of 26.32 W is stable. The output wavelength is 444.29 nm, the spectral linewidth is narrowed to 0.18 nm, and the fiber coupling efficiency reaches 88.1%. Further experimental studies will be conducted to reduce coupling loss and improve spectral locking quality, and then combined with spectral beam combination technology, higher power blue semiconductor lasers will be obtained.

Key words lasers; blue diode laser; narrow linewidth; volume Bragg grating; external cavity feedback